Bianchi, E., R. Villalba, M. Viale, et al., 2015: New precipitation and temperature grids for northern Patagonia: Advances in relation to global climate grids. *J. Meteor. Res.*, **29**(6), XXX－XXX, doi: 10.1007/s13351-015-5058-y. (in press)

New Precipitation and Temperature Grids for Northern Patagonia: Advances in Relation to Global Climate Grids

BIANCHI Emilio[1,2], VILLALBA Ricardo[3], VIALE Maximiliano[3], COUVREUX Fleur[3], and MARTICORENA Rocio[5]

1 *Instituto Nacional de Tecnología Agropecuaria (INTA), Estación Experimental Agropecuaria Bariloche. Modesta Victoria 4450, Bariloche, Argentina*

2 *Consejo Nacional de Investigaciones Científicas y Técnicas, Argentina*

3 *Instituto Argentino de Nivología, Glaciología y Ciencias Ambientales –CONICET, Mendoza. Ruiz Leal, Mendoza, Argentina*

4 *Centre National de Recherches Météorologiques (CNRM-GAME), Météo-France, Toulouse, France*

5. *Autoridad Interjurisdiccional de Cuencas, Argentina*

(Received July 1, 2015; in final form October 10, 2015)

Supported by 1) Instituto Nacional de Tecnología Agropecuaria (INTA), 2) Consejo Nacional de Investigaciones Científicas y Técnicas (CONICET), 3) the Australian Research Council (ARC DP120104320) and 4) Inter-American institute for Global Change Research (IAI), CRN02-47.

Corresponding author: bianchi.emilio@inta.gob.ar.

ABSTRACT

Climate data compiled from different sources in Northern Patagonia were interpolated to 20 km resolution grids of mean monthly temperature and total monthly precipitation over the period 1997-2010. This Northern Patagonia Climate Grid (NPCG) improves on previous gridded products in its spatial resolution and the number of contributing stations, since it incorporates 218 and 114 precipitation and temperature records, respectively. A geostatistical method using surface elevation from a Digital Elevation Model as ancillary variable was used to interpolate station data into even spaced points. The maps provided by NPCG are consistent with the broad spatial and temporal patterns of northern Patagonia climate, showing a comprehensive representation of the latitudinal and altitudinal gradients in temperature and precipitation, as well their related patterns of seasonality and continentality. We compared the performance of NPCG and other different data sets available to the climate community for northern Patagonia. The grids used for the comparison included the Global Precipitation Climatology Project (GPCP), the ERA-I reanalysis, the Climate Research Unit (CRU) from University of East Anglia and the University of Delaware (UDEL). NPCG outperforms other global grids based on BIAS, MAE and RMSE, three statistics that quantitatively assess the spatial coherence of gridded data against available observations. NPCG represents a useful tool for understanding climate variability in northern Patagonia and a valuable input for regional models of hydrological and ecological processes. Its resolution is optimal to validate data from the General Circulation Models (GCM) and for working with raster data derived from remote sensors such as vegetation indices.

Keywords: northern Patagonia, precipitation, temperature, co-kriging, climate grids, Cordillera de los Andes

1. Introduction

The low density of meteorological stations and the lack of temporal continuity in the records represent major limitations for climate research in South America (Castro et al., 2013; Garreaud et al. 2009; Schwerdtfeger, 1976). These limitations are even more pronounced in remote areas of the continent with reduced population and poor infrastructure such as the Patagonian region of Argentina and Chile (Fig. 1a, e.g., Garreaud et al. 2009; Viale and Garreaud, 2015; Villalba et al., 2003). A common alternative to overcome these limitations is to use global gridded climate datasets (e.g., re-analysis), which typically assimilate observations from the Global Climate Observing System (GCOS) using General Circulation Models (GCMs). However, the few conventional Patagonian stations included in the GCOS (Fig.1b) seriously limit the climate representation of these global gridded datasets over the complex topography in the region. Indeed, the climatic features in northern Patagonia are strongly modulated by the mountainous topography of the Cordillera de los Andes (Rusticucci et al., 2014).

A valid alternative to deal with the scarcity of conventional observations for climate researches (i.e., from GCOS) is to compile and assimilate additional observations from stations not included in global databases. The number these "nonconventional" weather stations, which do not belong to the National Weather Services of Argentina and Chile, has largely increased in the last decades over northern Patagonia as a result of isolated efforts of local and regional governmental institutions. Several regional agricultural institutions and water and energy management agencies have recently installed surface weather station networks for their own climatic monitoring. In this study, we compiled and assimilated these new surface observation networks to improve, together with conventional observations, the high-resolution spatial representation of climatic features over the Northern Patagonia region.

The development of the new regional monthly precipitation and temperature grids and their assessments for northern Patagonia are described here. A more realistic representation of the spatial distribution of temperature and precipitation over the Andes and their surroundings by these new regional grid is expected, so that it will help to improve the certainty of climatic, hydrologic and ecological studies in the region. They may also facilitate regional studies relating climate and vegetation attributes derived from remote sensors such as the Leaf Area Index (LAI) or the Normalized Difference Vegetation Index (NDVI; Bao et al., 2015; Fleming et al., 2000). Although the period considered is not long (14 years from 1997 to 2010), it allows incorporating the greatest number of records within the domain. A total of 218 precipitation and 112 temperature records were considered- which represent a considerable improvement compared to the network used by global climate grids (Fig. 2). Furthermore, the selected period of time includes singular climatic events, such as the 1998 regional drought, which is the most severe drought event recorded in the instrumental period over the past 100 years (Masiokas et al., 2008; Villalba et al., 2005). It also covers the 1997/1998 Southern Oscillation extremes encompassing the most intense El Niño-La Niña events recorded both in the instrumental record and in long-term climate reconstructions (Mann et al, 2000).

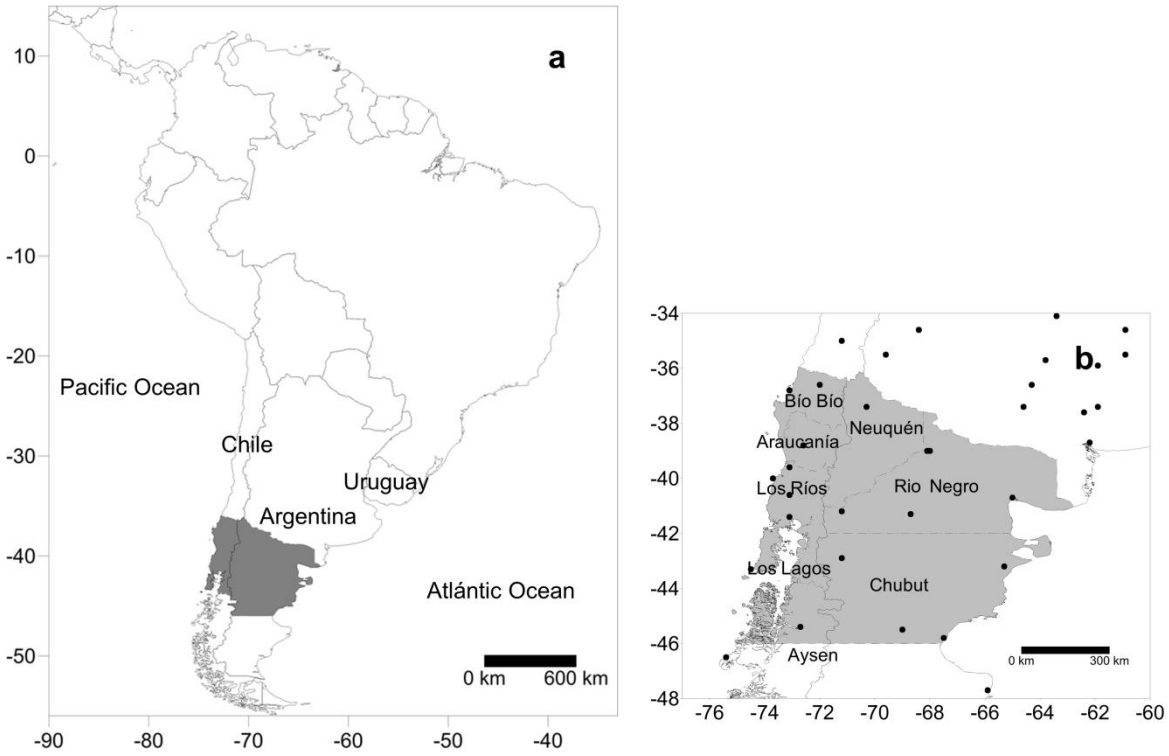

Fig. 1. (a) Location of the study area (shaded sector) and (b) meteorological stations included in the Global Climate Observing System (GCOS). The names of the Argentinean provinces and the Chilean regions in northern Patagonia are also indicated.

2. Materials and methods

2.1 Study area

The northern Patagonia region, which includes the Argentinean provinces of Neuquén, Río Negro and Chubut, and the Chilean regions of Bío Bío, Araucanía, Los Ríos, Los Lagos and Aysen (Fig. 1), is under the permanent influence of the Westerlies (Garreaud et al., 2009). The Westerlies determine the advection of humid air masses from the Pacific Ocean over the continent throughout the year. The bulk of the annual precipitation occurs in autumn and winter months, and its occurrence is related to more

frequent passages of transient low pressure systems during these seasons. Due to the main north–south orientation, the Cordillera de los Andes represents a major natural barrier for the humid air masses approaching the continent along the storm track trajectories. The cyclonic precipitation is augmented by the ascent of the air masses along the mountain slopes (Garreaud, 2009; Villalba et al., 2003). Consequently, regional precipitation maxima are recorded over both the Cordillera de los Andes and the Cordillera de la Costa (Falvey and Garreaud 2007; Viale and Nuñez, 2011; Viale and Garreaud, 2015).

The strong cross-barrier gradients generated by the topography are clearly reflected in the vegetation distribution (Paruelo et al., 1998).Total annual precipitation over the Cordilleras generally exceeds 2000-4000 mm and are associated with the presence of the Valdivian evergreen rainforest (Pisano, 1950; Donoso Zegers, 1993). Other forest types such as pure stands of Nothofagus sp. (Laclau, 1997), occur in sites where annual precipitation ranges between 1000 and 2000 mm. The relative importance of the cyclonic precipitation coming from the Pacific Ocean diminishes to the east. Most of the humidity brings by the Pacific maritime air masses is lost as precipitation during the ascent along the slopes of the Andes. In consequence, these air masses undergo adiabatic heating and drying over the leeside downslopes of the Andes (Garreaud, 2009). The narrow longitudinal band where annual precipitation decreases from 1000 to 500 mm coincides with a transition from different mesic forest types (mainly Araucaria araucana, Austrocedrus chilensis and Nothofagus sp.) to grass dominated steppes (Leon et al. 1998; Schlichter y Laclau, 1998). Farther east from the Andes, annual precipitation continues decreasing to totalize less than 200 mm in the Central Patagonian Plateau. This region is dominated by shrubby steppes associated with the transition between the Patagonia and Monte phytogeographical domains (Leon et al. 1998). Over the Atlantic coast, air masses from the Atlantic Ocean, with dominant northeastern direction, contribute with sporadic convective precipitation mainly in summer and early autumn. Thus, total annual precipitation increases from a minimum in the Central Patagonian Plateau to the northeast of the study area, reaching approximately 400 mm per year (Godagnone and Bran, 2008; Labraga and Villalba, 2009). Shrubby vegetation and C4-type grasses dominate this coastal region (Leon et al., 1998).

The spatial temperature pattern in the region is mainly determined by the north-south latitudinal gradient and the elevation (Villalba et al., 2003). Different atmospheric and oceanic circulation features also contribute to the regional temperature pattern (Garreaud et al., 2009). Alongside the Pacific coast, the Humboldt Cold Current intensifies the upwelling of deep cold waters which cool the lowest levels of the troposphere. On the Atlantic sector, the semi-permanent anticyclone over the South Atlantic Ocean advects warm, tropical maritime air masses to the region. The Cordillera de los Andes also introduces changes in the spatial pattern of temperature by means of the adiabatic heating release by the Pacific air masses on their descent paths from the mountains. Annual and daily temperatures reach the largest thermal amplitudes in the Central Patagonian Plateau, consistent with its location far apart from both the Pacific and Atlantic Oceans. As a consequence of the mentioned features, isotherms are oriented in a dominant northwest–southeast direction. Mean annual temperature ranges from 14 ℃ in the northeast to 10 ℃ in the southwest, with minima of about 6 ℃ in the high elevations of the Andes. The annual thermal amplitude ranges from 16 ℃ in the center of the Central Patagonian Plateau to about 10 ℃ in the southwest, near the Pacific coast (Garreaud et al., 2009; Paruelo et al., 1998).

2.2 Surface precipitation and temperature data

Monthly temperature and precipitation data were compiled for the region from different sources in Argentina and Chile. The Argentinean records were provided by 1) Servicio Meteorológico Nacional, 2) Instituto Nacional de Tecnología Agropecuaria, 3) Centro Nacional Patagónico (CONICET), 4) Departamento Provincial de Aguas (Río Negro), and 5) Autoridad Interjurisdiccional de Cuencas; whereas the Chilean sources of climate data included the 1) Dirección Meteorológica de Chile and 2) Dirección General de Aguas. This compilation, covering the period 1997-2010, includes 218 and 114 precipitation and temperature records, respectively (Fig. 2). Although a larger number of meteorological records were compiled, those records with more than 15 % of missing data were discarded from our study.

The temporal consistency of the station records was assessed using Principal Component Analysis (PCA; MacQueen, 1967; Navarra y Simoncini, 2010). By applying PCA, climate records were grouped accordingly to their geographical similarities. If a subset of regional records shows similar temporal patterns, they will likely belong to the same group. We targeted records as suspicious if they were not included in the group composed by their close neighbouring records. After targeting suspicious records, the lack of homogeneity was tested fitting double mass curves with the closest four stations in order to confirm the inhomogeneity of the record (e.g. in Fig. 3; Buishand, 1982). Non-homogeneous records were excluded from the pool of records to be gridded. Eight and six precipitation and temperature series, respectively, were rejected from our database. Figure 2 shows the terrain elevation derived from the Aster DEM along with the distributions of the precipitation and temperature records selected for gridding.

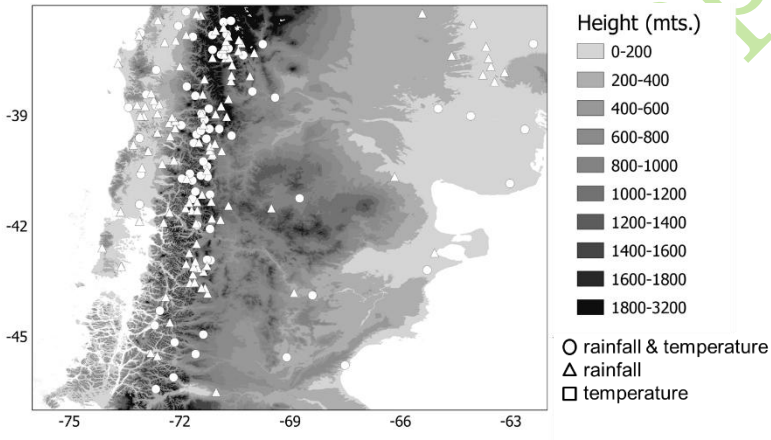

Fig. 2. Terrain elevation in Northern Patagonia derived from the Aster Digital Elevation Model (DEM) and spatial distribution of precipitation and temperature records.

The selected meteorological records are unevenly distributed across the region and mostly concentrated along to the Cordillera de los Andes. This uneven distribution reflects the density of the population across the region and the increasing number of meteorological stations in the upper catchments of the Andes installed by the hydroelectric power generation companies. In the Andes, changes in elevation greatly affect the spatial fields of climate. Therefore, a higher density of records in this sector is beneficial for a better

representation of the strong environmental gradients associated with the Cordillera. The density of meteorological records is lower to the east of 70 ºW; however, changes in terrain elevation are less abrupt in the eastern than in the western sector. In these topographically uniform eastern terrains, precipitation and temperature fields show more gradual gradients than in the western mountainous areas.

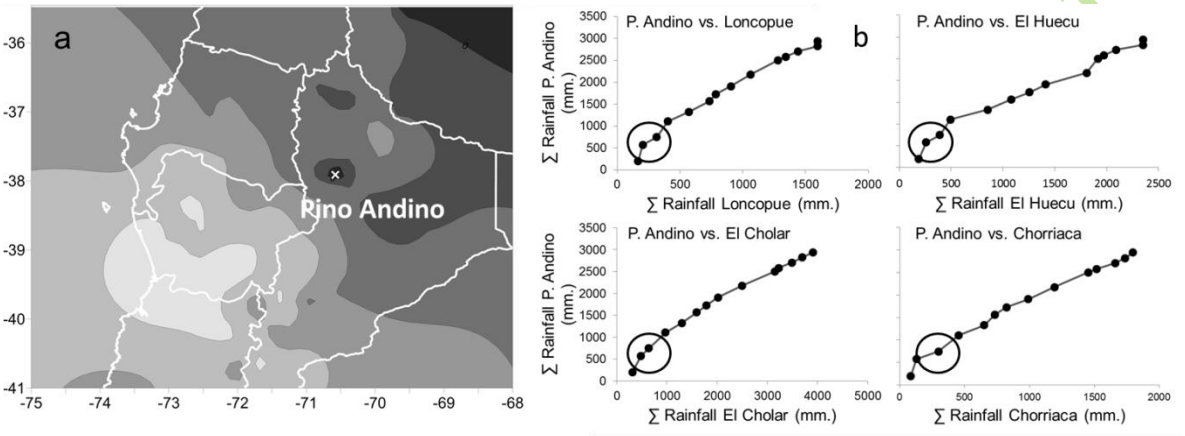

Fig. 3. (a) Spatial representation of PC2 loadings of winter (JJA) rainfall. The cross identifies a "suspicious" station. (b) Double mass curves between the suspicious station Pino Andino and the closest four stations. Stations with similar patterns of variability show straight lines connecting the accumulated values. A break in the trend (red circle) indicates an inconsistency in the record from the suspicious station.

2.3 Spatial fields of temperature and precipitation

The interpolation techniques commonly used to estimate spatial fields are diverse and they can roughly be classified as deterministic or geostatistical. The main difference between these two families of interpolation techniques resides in the criterion used to assign the interpolation weights. In deterministic methods, the interpolation weights depend on the geometric distance between points, whereas geostatistical methods (also called Kriging or Optimal Interpolation) use the semi-variance functions for weight estimations (Hartkamp et. al, 1999; Cressie, 1990; Gallardo & Maestre, 2008).

The use of geostatistical methods for data interpolation facilitates the incorporation of ancillary variables, such as elevation, in the interpolation of the primary variables (Baird, 1999). In our case the primary variables are temperature and precipitation. This type of geostatistical methods, called co-kriging, makes use of the relationship between the ancillary variable and those of interest (Goovaerts, 1998; Isaaks & Srivastava, 1989). For example, rainfall generally increases with elevation in response to orographic effects whereas temperature decreases with elevation according to the lapse rate in the atmosphere (Barry, 2013; Castro et al., 2014). Based on these relations, several authors have used elevation as a secondary variable to interpolate precipitation and temperature data using co-kriging techniques (Goovaerts, 2000; Ishida & Kawashima, 1993; Sarangi et al., 2005). Here, we used ordinary co-kriging (Goovaerts, 1998) to transform unevenly distributed monthly rainfall and temperature observations into regular 20 x 20 km resolution grids. Elevation, derived from the ASTER Digital Elevation Model, was used as the ancillary variable. The DEM was degraded from its original 30 m x 30 m resolution to a 20 km x 20 km resolution in order to match the climate grids (Fig. 2).

For the interpolation of the meteorological data, the search area was divided into four quadrants, retaining in each quadrant, a minimum of two and a maximum of five stations to be included in the interpolation. Since rainfall events and air mass intrusions on a monthly scale are superimposed on the long-term gradients associated with topography, anisotropy was not considered.

2.4 Inter-comparison with global climate grids

The performance of NPCG fields was compared with global climate grids using cross-validation techniques between observed and gridded data. We computed the residual metrics BIAS (equation 1), Mean Absolute Error (MAE, equation 2) and Root Mean Squared Error (equation 3; Isaaks and Srivastava, 1989) between the station observations and their respective nearest grid points. BIAS indicates whether a grid under or over estimates an observed variable, whereas MAE and RMSE are a measure of the absolute error. BIAS, MAE and RMSE statistics are defined as follows:

$$BIAS = \frac{1}{n}\sum_{i=1}^{n} r \quad (1)$$

$$Mean\ Absolute\ Error\ (MAE) = \frac{1}{n}\sum_{i=1}^{n} |r| \quad (2)$$

$$Root\ Mean\ Squared\ Error\ (RMSE) = \sqrt{\frac{1}{n}\sum_{i=1}^{n} r^2} \quad (3)$$

Where:

$$r = error = x' - x \quad (4)$$

$n = number\ of\ observational\ data$

$\acute{x} = the\ closest\ grid\ point\ estimation\ to\ the\ observational\ data$

$x = observational\ data$

To assess the NPCG quality, we used a cross-validation procedure, in which x represents the observed values, and x' represents the estimated values. In a cross-validation procedure, an observed value at a particular location is temporarily discarded from the interpolation. The value at the same location is then estimated using the remaining observed values. The process is repeated for all the observed values. This procedure allows evaluating the fitness between the grids and the observed data as if they were independent of each other.

The global climate data sets selected for inter-comparisons with NPCG were:

1. Climate Research Unit (CRU), University of East Anglia: CRU TS3.21 (Harris et al, 2014). Temperature and precipitation gridded monthly, 0.5 °X 0.5 °resolution data
2. University of Delaware (UDEL), 3.01 version. Temperature and precipitation gridded monthly, 0.5 °X 0.5 °resolution data.
3. Global Precipitation Climatology Project (GPCP). Precipitation gridded monthly, 1 ° X 1 ° resolution data. Combines ground observations with satellite estimations (Adler et al., 2003).
4. ERA-interim reanalysis. Temperature gridded monthly 0.75 ° X 0.75 ° resolution data (Berrisford et al., 2011).

Finally, we compared the temporal evolution of rainfall and temperature for the different gridded data sets computed as spatial means of monthly temperature and rainfall east and

west of the Andes following the 71 ℃W meridian. Monthly time series for both sectors were visually inspected and the relationships between station and gridded data sets were tested using Pearson's correlation coefficients.

3. Results

3.1 Representation of spatial patterns

3.1.1 Precipitation spatial fields

Figure 4 shows the mean annual precipitation for the different gridded data sets, whereas Figure 5 displays precipitation variations along longitudinal transects at 38 ℃S, 41 ℃S and 44 ℃S. The most salient feature in the mean precipitation fields is the strong gradient across the Andes associated with the mountainous orography. This precipitation pattern is reproduced more realistically by the new regional NPCG grid than the global grids. The new NPCG grid shows a well-defined maximum all along the windward slopes of the Cordillera de los Andes west of the continental divide (located approximately at the Argentinean-Chilean border) and a strong cross-barrier gradient (Figs. 4d and 5). In contrast, the global grids reproduce either isolated maximum or no maximum on the windward slopes and weaker cross-barrier gradients (Figs. 4a-b, and 5). NPCG shows the steepest decrease of rainfall on the lee side of the Andes reflecting the strong rain-shadow effect. In the NPCG regional-derived map, precipitation spills over the Andes up to a distance of ~100 km to the east of the crest (Fig. 4d), whereas in their global-derived counterparts, it extends to ~200-300 km from the crest (Figs. 4a-c).

The NPCG shows the best validation statistics (Fig. 4), which further support its more realistic estimates of orographic precipitation pattern compared with those from global grids. Even though all grids show a negative BIAS, the NPCG show the smallest value as well as the lowest MAE and RMSE, all indicative of a reduced dispersion of the errors.

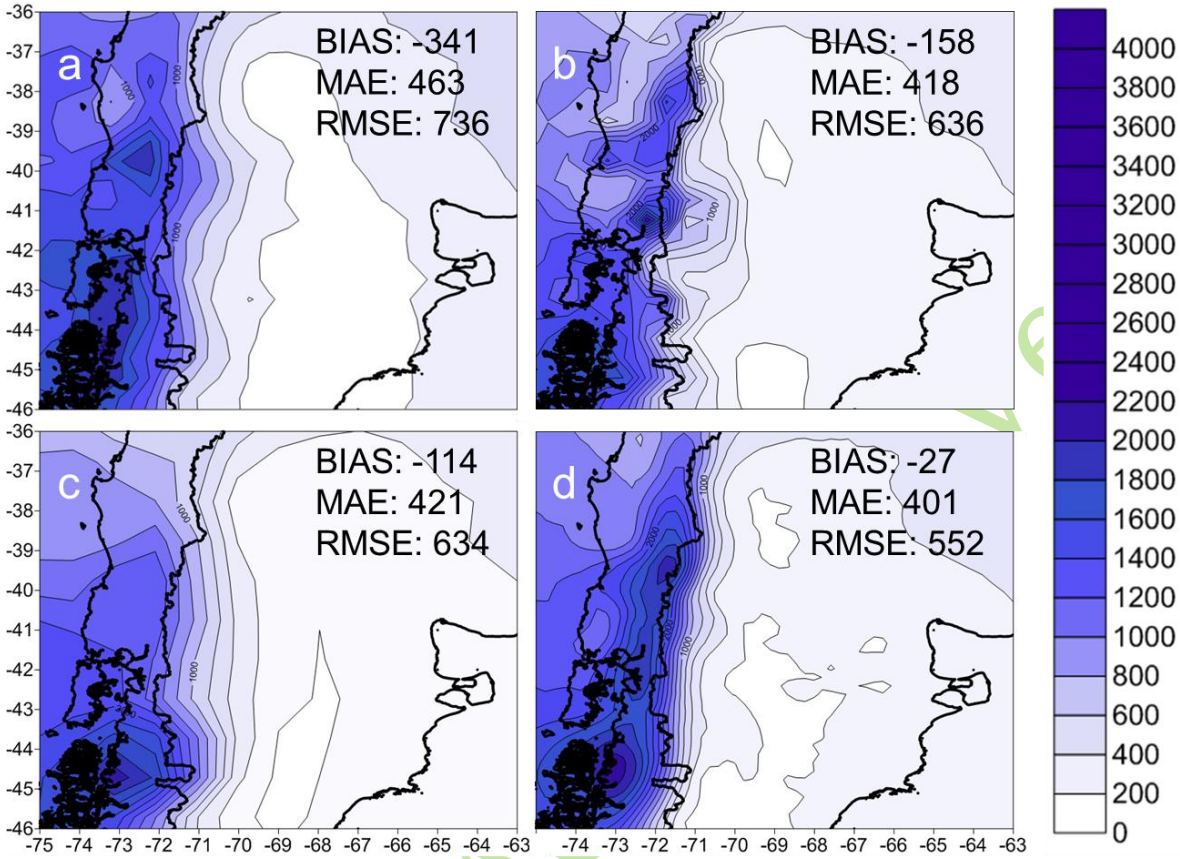

Fig. 4. Mean annual precipitation (mm) according to the following gridded data: CRU (a), UDEL (b), GPCP (c), and NPCG (d). BIAS, MAE and RMSE statistics are provided for each field.

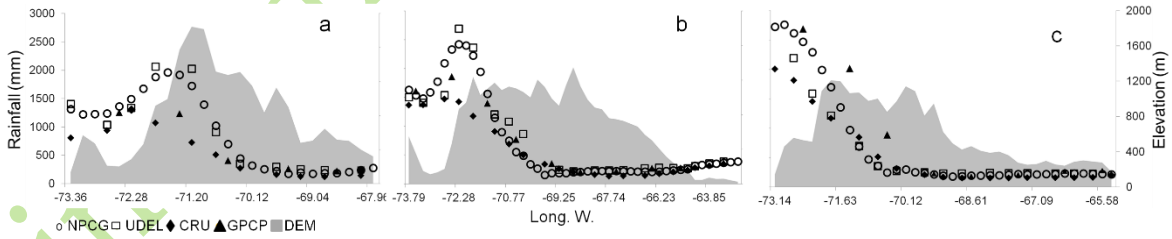

Fig. 5. Longitudinal transects of total annual precipitation at 38 ℃S (a), 41 ℃S (b) and 44 ℃S (c). The topography along the respective transects is indicated by grey shaded areas.

3.1.2 Temperature spatial fields

Figure 6 shows the mean annual temperature fields for the selected gridded data sets, whereas Fig. 7 portrays temperature variations across longitudinal transects at 38 ℃S, 41 ℃S and 44 ℃S. Temperature exhibits a close relationship with elevation since the lowest temperatures are consistent with the highest elevations along the crest of the Andes (indicated approximately by the Argentinean-Chilean border) and the elevated Northern Patagonian Plateau. In contrast, the warmer temperatures are recorded at the low-elevation sectors of the study area. This interrelationship between temperature and elevation is superimposed on the regional northeast-southwest temperature gradient. Along the 38 ℃S transect (Fig. 7a), NPCG, CRU and UDEL show local minima over the Cordillera de la Costa and Cordillera de los Andes and a local maximum over the Central Valley of Chile. UDEL shows lower temperatures in the upper Andes than the global grids. Estimated NPCG temperatures are above the other global grids. From the easternmost extreme of the our study region to till 67 ℃W, temperature differences between NPCG and other grids are close to 2 ℃ and increase to about 4 ℃ between 71 ° and 71.5 ℃W.

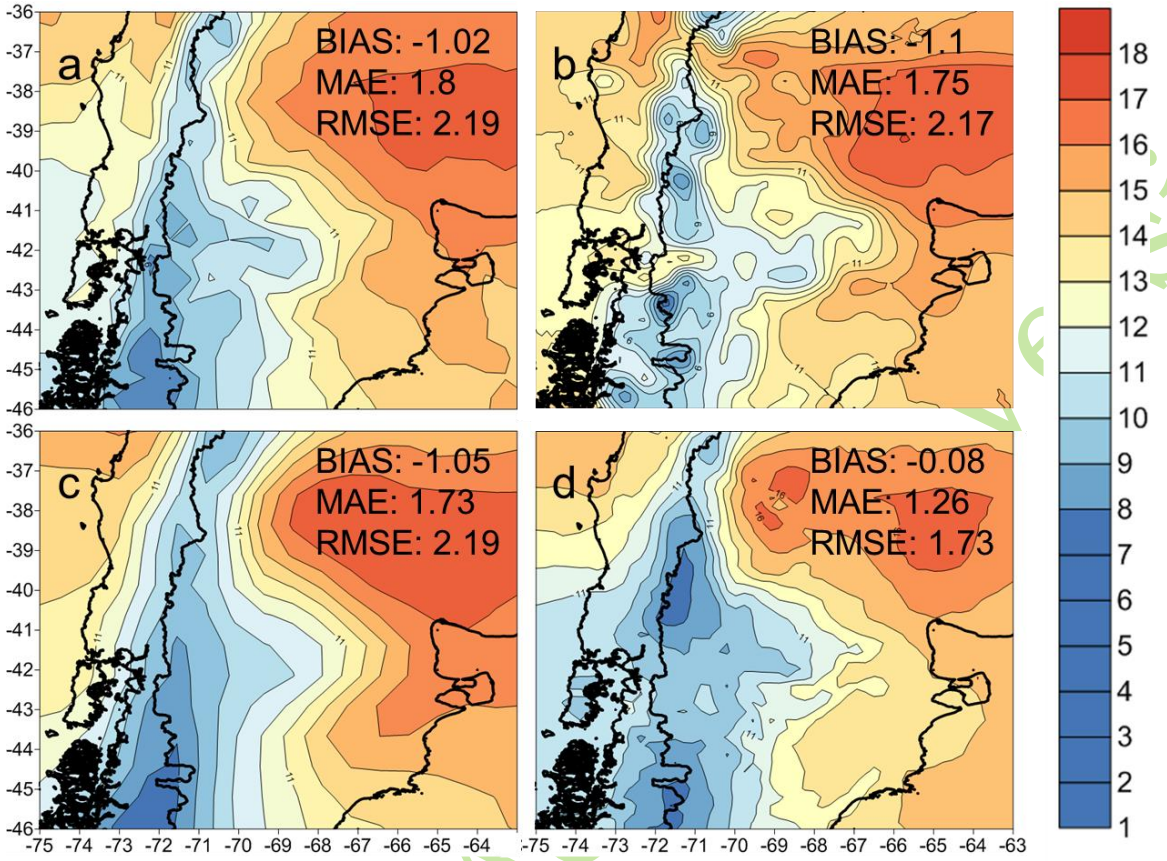

Fig. 6. Mean annual temperature (℃) according to CRU (a), UDEL (b), ERA (c) and NPCG (d). BIAS, MAE and RMSE statistics are shown for each field.

Similar to precipitation spatial fields, the UDEL spatial pattern of temperature is highly perturbed across the Cordillera de los Andes. NPCG shows the smallest BIAS, MAE and RMSE statistics followed by ERA and CRU, respectively.

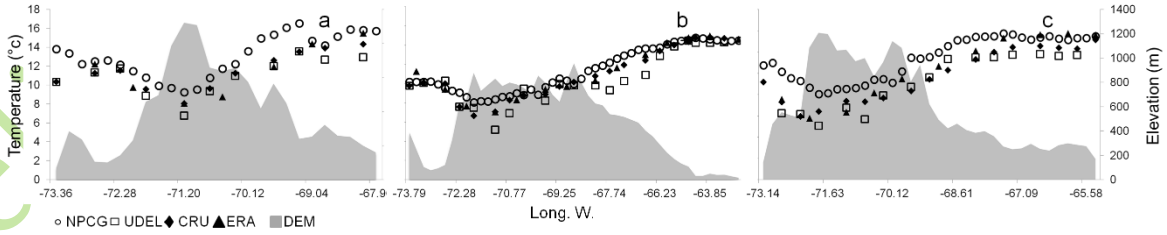

Fig. 7. Longitudinal transects of mean annual temperature at 38 ℃S (a), 41 ℃S (b) and 44 ℃S (c).

3.2 Representation of temporal variations

3.2.1 Precipitation

Monthly precipitation variations over the interval 1997-2010 are shown in Figure 8 for the sectors east and west of 71 °W (i.e., east and west of the Andes). Broadly, all series show similar variations at inter and intra annual time scales. Precipitation series on the western side of the Andes show a more pronounced annual cycle than those on the eastern side. By comparison with global grids, the NPCG generally shows the most contrasting precipitation variations between the sectors located west and east of the Andes. Precipitation maxima west of 71 ºW are larger in NPCG than at any other grid. On the contrary, values of NPCG east of 71 ºW are generally below those from other grids. These results are in line with a better orographic precipitation representation by the NPCG compared to those from the global grids. NPCG provides a more realistic precipitation enhancement on the windward slopes as well as a more pronouced rain shadow effect on the downslopes of the Andes. In contrast, GPCP presents the lowest precipitation maxima to the west of the crest and the highest precipitation minima to the east of the crest of the Andes, as a consecuence of its poor orographic precipitation representation.

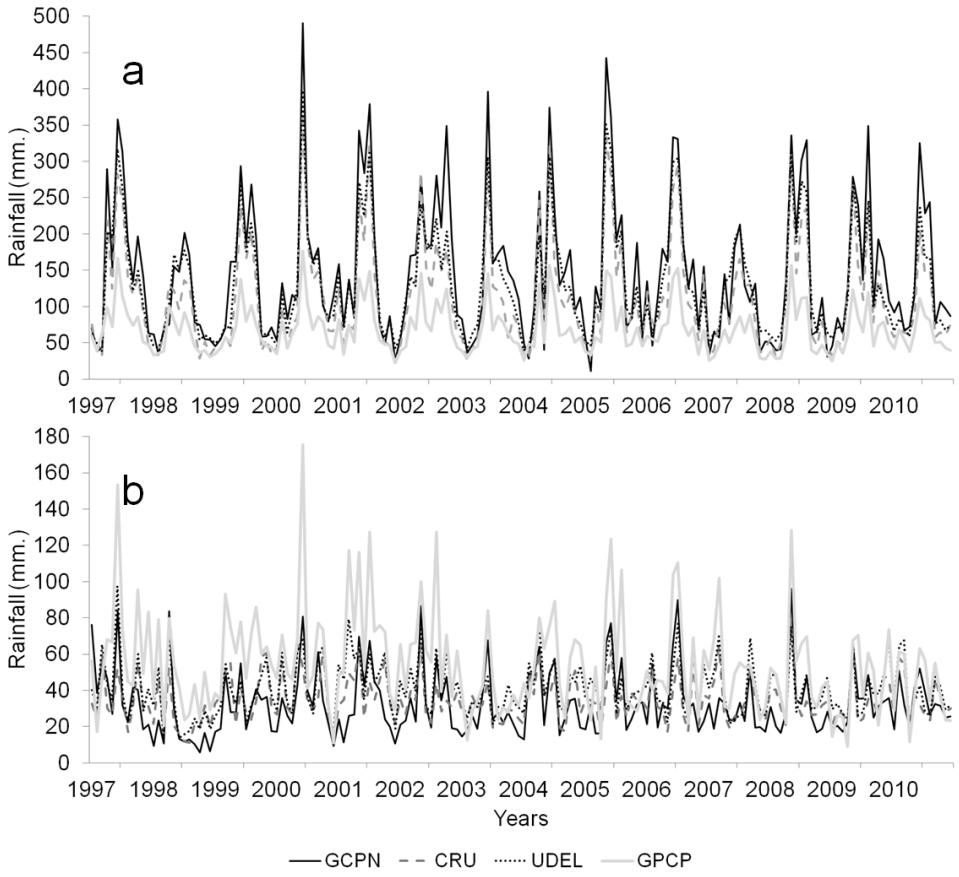

Fig. 8. Monthly total precipitation averaged over the sectors located west (a) and east (b) of 71 ºW.

Table 1 shows the correlation coefficients between the precipitation series from different grids west and east of 71 ° W. The temporal evolution of the series is more homogeneous west of 71 ° W than in their eastern counterparts, probably due to the dominant stratiform type of western precipitation, whereas mostly localized, convective precipitation occurs on the eastern side during the warm season. The GPCP grid shows the weakest relationships with the other grids. Correlation coefficients estimated for the precipitation anomalies (annual cycle removed) show the same overall pattern (Table 1b).

Table 1. Correlation matrices between monthly precipitation (a) and monthly precipitation anomalies (b) between different grids averaged west (left) and east (right) of Andes (71 °

W). All correlation coefficients, estimated over the interval January 1997 to December 2010, are statistically significant at 99.9% confidence level.

a)

West	UDEL	GPCP	NPCG	East	UDEL	GPCP	NPCG
CRU	0.97	0.64	0.95	CRU	0.88	0.38	0.65
UDEL	-	0.62	0.96	UDEL	-	0.50	0.71
GPCP		-	0.60	GPCP		-	0.79

b)

West	UDEL	GPCP	NPCG	East	UDEL	GPCP	NPCG
CRU	0.94	0.58	0.90	CRU	0.87	0.56	0.72
UDEL	-	0.58	0.94	UDEL	-	0.72	0.78
GPCP		-	0.51	GPCP		-	0.77

3.2.2 Temperature

The time series of monthly temperatures for the western and eastern sectors of the study region are depicted in Figure 9. All grids show a similar representation of the annual cycle in both sectors. In the western sector, the series display the largest differences between grids. NPCG shows a wider annual cycle than the other grids with maxima between 2 °C and 3 °C warmer and minima around 1 °C colder than global grids, consistent with a large number of station records, a better representation of the topography and their influences on temperature.

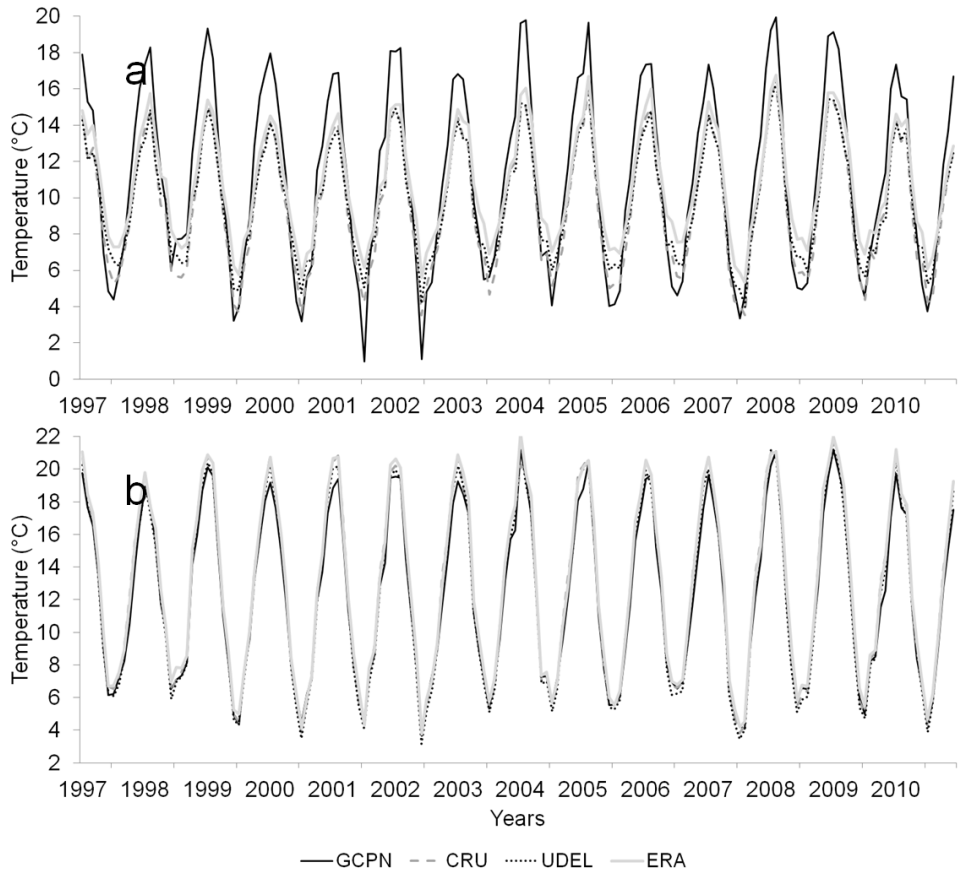

Fig. 9. Mean monthly temperature spatially averaged for the sectors located west (a) and east (b) of 71 °W.

All correlation coefficients between grids are statistically significant, slightly lower for NPGC at the west than at the east of 71 °S (Table 2). Temperature differences between NPCG and the other grids are more marked when the mean annual cycle is subtracted from the records (Table 2, b)

Table 2. Correlation matrices between monthly temperature (a) and monthly temperature anomalies (b) for the different grids averaged west (left) and east (right) of 71 °W. All correlation coefficients are statistically significant at 99.9% confidence level.

a)								b)							
West	UDEL	ERA	NPCG	East	UDEL	ERA	NPCG	West	UDEL	ERA	NPCG	East	UDEL	ERA	NPCG

CRU	0.99	0.99	0.98	CRU	0.99	0.99	0.99	CRU	0.96	0.96	0.78	CRU	0.97	0.96	0.92
UDEL	-	0.99	0.98	UDEL	-	0.99	0.99	UDEL	-	0.95	0.81	UDEL	-	0.97	0.94
ERA		-	0.97	ERA		-	0.99	ERA		-	0.81	ERA		-	0.95

4. Discussion and conclusions

Interactions between topography, atmospheric circulation and proximity to the oceans introduce large complexities in the spatial patterns of precipitation and temperature in northern Patagonia. The Cordillera de los Andes acts as a formidable barrier to the atmospheric circulation in the South America and generates not only strong climatic gradients but also synoptic and meso-scale atmospheric perturbations in both Andean slopes (e.g. Falvey and Garreaud 2007; Viale and Nuñez 2011; Barrett et al., 2009; Garreaud, 2009; Viale et. al 2013). Moist maritime cross-barrier flow produces precipitation maxima up to 4000 mm on the western slopes of the Andes (Viale and Garreaud, 2015). Over the eastern slopes, the rain shadow effect modulates an exponential decrease in annual rainfall reaching less than 200 mm in the Central Plateau, located aprox. 60 km east from the major Andes peaks (Jobbagy et al., 1995).

The Andes topography also affects the spatial patterns of temperature through its interactions with the atmospheric lapse rate (Barry, 2013). Temperature generally decreases with elevation, but in some cases, stable and cold air masses produce inversions in the boundary layer (Oke, 2002). Topography also influences temperature patterns by blocking atmospheric circulation and reducing the pass of air masses across the main Andean barrier. In that sense, Falvey and Garreaud (2009) and Villalba et al. (2003) have documented opposite temperature trends in the west and east slopes of the Andes.

Given this complexity in precipitation and temperature spatial patterns, the low number of meteorological stations from northern Patagonia included in the global GCOS data set (Fig. 1) largely reduces the abilities of global grids to capture local and regional features of climate variability. Regional climate grids need to be improved by including additional climate observations in the region. Based on climatic records from governmental and

private institutions in northern Patagonia, we compiled climatic information from 218 precipitation and 114 temperature stations, which represent a significant increase in the number of records included in the conventional GCOS data set. Our data set was co-kriged using terrain elevation as the ancillary variable, to obtain 20 km x 20 km grids of precipitation and temperature in Northern Patagonia. This new regional NPCG grid represents more realistic spatial features of the mean fields of precipitation and temperature than the commonly used global gridded datasets.

We compared the new NPCG with global gridded climate data sets commonly used in the region. Comparisons were performed for mean spatial fields and monthly variations in temperature and precipitation over the interval 1997-2010. NPCG represents more accurately the rainfall and temperature gradients on both slopes of the Andes (e.g. the decrease (increase) of rainfall (temperature) in the Central Valley of Chile, and the increase of rainfall from the Central Patagonian Plateau towards the Atlantic coast) than other gridded data sets. NPCG and UDEL perform better in representing the spatial variability of rainfall associated with topography (e.g. the decrease of rainfall in the Central Valley of Chile), probably due to the higher spatial resolution of both data set. However, UDEL shows some inconsistences on the spatial patterns over the Andes due to the limited number of stations included in this data set for the region. For temperature, the gridded data sets with the higher resolution grids (NPCG, UDEL, CRU) perform better in representing spatial features than ERA, whose resolution is 0.75°. We used the BIAS, MAE and RMSE statistics to assess the fitness of the different grids to the observed data. Based on these statistics, NPCG performs better than other grids in both temperature and precipitation spatial fields. The other grids showed similar statistics between them. Although the temporal evolution of precipitation and temperature is similar between grids and shows similar spectral properties (not shown), there are significant differences in the amplitude of the annual cycle of NPCG and global grid products. Larger amplitudes in the annual cycle of temperature, particularly for the eastern sector of the study region, should be related to the larger number of records included and the small radios of 20 km x 20 km used for the interpolation of the grid cells in NPCG. Differences in temperature ranging from 2 to 4 ℃

between NPCG and other global gridded products shows the relevance of including as many stations as possible in regions with steep environmental gradients as northern Patagonia.

A main difficulty found in gridding climate data at regional scale in northern Patagonia deals with differences in the interactions of elevation with rainfall and temperature for different sub-regions (mountains vs. relative flat plateaus and lowlands). The strong north-to-south oriented gradients associated with the Cordillera de los Andes contrast with the relatively smoothed gradients in the Central Patagonian Plateau. Rainfall and temperature variations with elevation are modulated by interactions between the atmospheric flow and the topography, which are extremely variable in the region. These features complicate the selection of the optimum interpolation parameters, as well as the variogram model, the anisotropy of the search neighbourhood radii, and the searching criterion.

Although the number of records included in our compilation greatly exceeds that included in the GCOS, its spatial density is still not high enough to represent local scale precipitation and temperature variations tied to the topography as the PRISM interpolation method does for the mountainous western US (Daly et al., 1994). The PRISM method allows representing fine scales of climatic variations as those associated with diurnal cycles between valleys and peaks. However, these high-resolution features of climate variability required basic climatic information from dense networks not currently available in northern Patagonia. Given the present density of climate records, the use of the co-kriging methodology, employing elevation as ancillary information, comparatively improve the representation of the spatial fields of precipitation and temperature across northern Patagonia.

Acknowledgments. Álvaro González provided additional climate data. Fernando Umaña provided assessment in the use of GIS software.

Reference

Adler, R. F., G. J. Huffman, A.Chang, R. Ferraro, et al., 2003: The version-2 global precipitation climatology project (GPCP) monthly precipitation analysis (1979-present). *J. Hydrometeor.*, **4**, 1147-1167.

Baird, A. J., and R.L. Wilby, 1999: Eco-Hydrology: Plants and water in terrestrial and aquatic environments. *Hydrological Sciences Journal-Journal des Sciences Hydrologiques*, **45**, 498-498.

Bao, G., Y, Bao, Sanjjava, A., et al., 2015: NDVI-indicated long-term vegetation dynamics in Mongolia and their response to climate change at biome scale. *Int. J. Climatol.* . doi: 10.1002/joc.4286, *http://onlinelibrary.wiley.com/doi/10.1002/joc.4286/full*.

Barrett, B. S., R. Garreaud, and M. Falvey, 2009: Effect of the Andes cordillera on precipitation from a midlatitude cold front. *Mon. Wea. Rev.*, **137**, 3092-3109.

Barry, R. G., 2013: *Mountain Weather and Climate*. Routledge. Cambridge University Press, Cambridge, 532 pp.

Berrisford, P., P. Kallberg, S. Kobayashi, et l., 2011b: The ERA-Interim Archive Version 2.0. European Centre for Medium-Range Weather Forecasts ERA Tech. Rep, **1**, 23 pp.

Buishand, T. A., 1982: Some methods for testing the homogeneity of rainfall records. *J. Hydrol.*, **58**, 11-27.

Castro, L. M., M. Miranda, and B. Fernández, 2015: Evaluation of TRMM Multi-satellite precipitation analysis (TMPA) in a mountainous region of the central Andes range with a Mediterranean climate. *Hydrology Research*, **46**, 89-105.

Castro, L. M., J. Gironás, and B. Fernández, 2014: Spatial estimation of daily precipitation in regions with complex relief and scarce data using terrain orientation. *J. Hydrol.*, **517**, 481-492.

Cressie, N., 1990: The origins of kriging. *Mathematical geology*, **22**, 239-252.

Daly, C., R.P. Neilson, and D.L. Phillips, 1994: A statistical-topographic model for mapping climatological precipitation over mountainous terrain. *J. Appl. Meteor.*, **33**, 140-158.

Falvey, M., and R. Garreaud, 2007: Wintertime precipitation episodes in Central Chile: associated meteorological conditions and orographic influences, *J. Hydrometeor.*, **8**, 171-193.

Falvey, M., and R. Garreaud, 2009: Regional cooling in a warming world: Recent temperature trends in the southeast Pacific and along the west coast of subtropical South America (1979–2006). *J. Geophys. Res. Atmos.* , **114**, 4102.

Fleming, M. D., F.S. Chapin, W. Cramer, et al., 2000: Geographic patterns and dynamics of Alaskan climate interpolated from a sparse station record. *Global Change Biology*, **6**(S1), 49-58.

Gallardo, A., and F.T. Maestre, 2008: Métodos geoestadísticos para el análisis de datos ecológicos espacialmente explícitos. *Introducción al análisis espacial de datos en ecología y ciencias ambientales: métodos y aplicaciones*, FT Maestre, A. Escudero y A. Bonet (eds.). Dykinson, Madrid, 215-272.

Garreaud, R., 2009: The Andes climate and weather. *Advances in Geosciences*, **22**, 3-11.

Garreaud, R. D., M. Vuille, R. Compagnucci, et al., 2009: Present-day South American climate. *Palaeogeography, Palaeoclimatology, Palaeoecology*, **281**, 180-195.

Godagnone, R., and D. Bran, 2009: Inventario integrado de los recursos naturales de la Provincia de Río Negro: geología, hidrogeología, geomorfología, suelo, clima, vegetación y fauna. Ediciones INTA, Buenos Aires, 392 pp.

Goovaerts, P., 1998: Ordinary cokriging revisited. *Mathematical Geology*, **30**, 21-42.

Goovaerts, P., 2000: Geostatistical approaches for incorporating elevation into the spatial interpolation of rainfall. *J. Hydrol.*, **228**, 113-129.

Harris, I., P. D. Jones, T.J. Osborn, et al., 2014: Updated high-resolution grids of monthly climatic observations–the CRU TS3.10 dataset. *Int. J. Climatol.*, **34**, 623-642.

Hartkamp, A.D., K.A. De Beurs, A. Stein, et al., 1999: Interpolation techniques for climate variables. CIMMYT. Series: CIMMYT NRG-GIS Series. Mexico, 26 pp.

Isaaks, E. H. and R.M. Srivastava, 1989: *An Introduction to Applied Geostatistics*. New York, Oxford University Press. 561 p.

Ishida, T. and S. Kawashima, 1993: Use of cokriging to estimate surface air temperature from elevation. *Theor. Appl. Climatol.*, **47**, 147-157.

Jobbágy, E. G., J.M. Paruelo, and R.J. León, 1995: Estimación del régimen de precipitación a partir de la distancia a la cordillera en el noroeste de la Patagonia. *Ecología Austral*, **5**, 47-53.

Kalnay, E., M. Kanamitsu, R. Kistler,et al., 1996: The NCEP/NCAR 40-year reanalysis project. *Bull. Amer. Meteor. Soc.*, **77**, 437-471.

Labraga, J. C., and R. Villalba, 2009: Climate in the Monte Desert: past trends, present conditions, and future projections. *Journal of Arid Environments*, **73**, 154-163.

Laclau, P., 1997: Los ecosistemas forestales y el hombre en el sur de Chile y Argentina. Boletín técnico, 34. Fundación Vida Silvestre Argentina, Buenos Aires, 147 p.

León, R., D. Bran, M. Collantes, et al., 1998: Main vegetation units of the extra andean Patagonia. *Ecología Austral*, **8**, 125-144.

MacQueen, J., 1967: Some methods for classification and analysis of multivariate observations. In Proceedings of the fifth Berkeley symposium on mathematical statistics and probability, **1**, 281-297.

Mann, M. E., R. S. Bradley, and M. K. Hughes, 2000: Long-term variability in the El Nino Southern Oscillation and associated teleconnections. Cambridge University Press, Cambridge, 357-412.

Masiokas, M. H., R. Villalba, B.H. Luckman, et al., 2008: 20th-century glacier recession and regional hydroclimatic changes in northwestern Patagonia. *Global and Planetary Change*, **60**, 85-100.

Navarra, A., and V. Simoncini., 2010: A guide to empirical orthogonal functions for climate data analysis. Springer, New York, 39-67.

Oke, T. R., 2002: Boundary Layer Climates. Routledge, Lonon, 435 pp.

Paruelo, J. M., E.G. Jobb ágy, and O.E. Sala, 1998a: Biozones of Patagonia (Argentina). *Ecolog ía Austral*, **8**, 145-153.

Paruelo, J. M., A. Beltran, E.G. Jobbagy, et al., 1998b: The climate of Patagonia: general patterns and controls on biotic. *Ecolog ía Austral*, **8**, 85-101.

Rusticucci, M., N. Zazulie, and G.B. Raga, 2014: Regional winter climate of the southern central Andes: Assessing the performance of ERA-Interim for climate studies. *J. Geophys. Res. Atmos.*, **119**, 8568-8582.

Sarangi, A., C.A. Cox,, and C.A. Madramootoo, 2005: Geostatistical methods for prediction of spatial variability of rainfall in a mountainous region. *Transactions of the American Society of Agricultural Engineers*, **48**, 943-954.

Schlichter, T., and P. Laclau, 1998: Ecotono estepa-bosque y plantaciones forestales en la Patagonia norte. *Ecolog ía Austral*, **8**, 285-296.

Schwerdtfeger, W., 1976: Climates of Central and South America, *World Survey of Climatology* Volume 12.. Elsevier Scientific Publishing, Amsterdam, 532 pp.

Viale, M., and M.N. Nuñez, 2011: Climatology of winter orographic precipitation over the Subtropical Central Andes and associated synoptic and regional characteristics, *J. Hydrometeor*., **12**, 481-507.

Viale, M., R. A. Jr. Houze, and K.L. Rasmussen, 2013: Upstream orographic enhancement of a narrow cold frontal rainband approaching the Andes, *Mon. Wea. Rev.*, **141**, 1708–1730.

Viale, M., and R. Garreaud, 2015: Orographic effects of the subtropical and extratropical Andes on upwind precipitating clouds, *J. Geophys. Res. Atmos.*, **120**, doi: 10.1002/2014JD023014.

Villalba, R., A. Lara, J.A. Boninsegna, et al., 2003: Large-scale temperature changes across the southern Andes: 20th-century variations in the context of the past 400 years. *Climatic Change*, **59**, 177-232.

Villalba, R., M.H. Masiokas, T. Kitzberger, et al., 2005: Biogeographical consequences of recent climate changes in the southern Andes of Argentina. *In: Global Changes and Mountain Regions.* U. Huber and M. Reasoner (eds.). Mountain Research Initiative, Switzerland. Springer, 157-168.

Donoso Zegers, C. D., 1993: Bosques templados de Chile y Argentina: variación, estructura y dinámica. Editorial Universitaria, Santiago de Chile, 483 pp.